

Original Article

Distributed Secondary Control in DC Microgrid for Voltage Restoration and Current Sharing

Shilpa Kaila¹, Rajnikant Bhesdadiya², Hitesh Karkar³

¹Department of Electrical Engineering, Gujarat Technological University, Gujarat, India.

²Department of Electrical Engineering, Lukhdhirji Engineering College, Gujarat, India.

³Department of Electrical Engineering, Government Engineering College, Rajkot, Gujarat, India.

¹Corresponding Author : shilpakaila28@gmail.com

Received: 09 February 2024

Revised: 10 March 2024

Accepted: 08 April 2024

Published: 30 April 2024

Abstract - In comparison to an AC system, a DC microgrid is becoming highly popular on account of its ease of connecting renewable energy resources, high reliability, and high efficiency. The primary goals of a DC microgrid are to retain a constant voltage on a DC bus and ensure appropriate current distribution amongst all converters. Proper current sharing can be accomplished with the traditional droop technique at the primary level of control. However, the DC output voltage of a converter decreases linearly with an increase in output current. It is a limitation of primary control. So, this work presents a secondary control approach based on the Low-Bandwidth Communication (LBC) network to enhance the function of the DC microgrids. It is implemented by using a local-level controller and the LBC link to transmit information. A secondary current controller is used in each converter module to increase the accuracy of current sharing, while a secondary voltage controller is used to retain the DC bus voltage at its nominal voltage. Every controller is implemented locally, and the LBC channel is just utilized to transmit DC current values. Because of this, the approach is appropriate for distributed microgrid control. Finally, MATLAB/Simulink software is utilized to validate the efficiency of a proposed distributed secondary control technique.

Keywords - DC microgrid, Primary control, Distributed control, Voltage restoration, Current sharing.

1. Introduction

These days, Renewable Energy Resources (RESs) like fuel cells, wind energy, and solar energy are very famous and are combined with the electrical power grid to function as Distributed Energy Resources (DERs) in an effort to reduce the severe environmental issues and global energy crises brought on by the use of fossil fuels [1, 2]. Energy storage apparatuses, Distributed Energy Resources (DERs), and loads are usually integrated to form the microgrids [3]. It can function either combined with the main power grid as a grid-connected mode of operation or independently as an islanded mode of operation [4]. Based on the type of bus voltage, it can be classified into three types: Direct Current (DC) microgrid, Alternating Current (AC) microgrid, and hybrid (AC-DC) microgrid. [5]. Consider the DC microgrid concept as the main basis for putting Smart Grid (SG) technologies into practice [6]. The majority of loads and Distributed Energy Resources (DERs) can directly connect to the DC bus, in contrast to an AC grid. Hence, DC microgrids provide excellent power quality, reliability, and efficiency. These benefits include,

1. No reactive power and harmonics.
2. Simple integration of several DERs and loads.

3. Fewer steps of power conversion.
4. Simple control without phase or frequency problems [7, 8].

The primary goals of connecting many DC converters parallel to a common DC bus are DC bus voltage regulation [9, 10] and the proper load current sharing ratio between converters [11, 12]. Droop control plays a vital role in ensuring current sharing in the primary control layer [13]. It is achieved by including a virtual resistance loop (droop) in the DC/DC converter's primary control loop [14]. Droop control can guarantee a proportional current distribution by taking the droop gain to be significantly bigger than the resistance of the line. Furthermore, since droop control has to be executed in a completely decentralized manner, there is no need for communication between the DC sources.

Nevertheless, as mentioned in [15], the voltage of the DC bus will significantly drop from the nominal voltage if a larger droop gain is specified in droop control. This shows that if just droop control is employed, voltage regulation of the DC bus and the accuracy of current sharing are not achieved simultaneously. Hence, complementary approaches must be developed to address the voltage violation issue brought on by



Equation 8 demonstrates how the droop gain affects the current sharing ratio. In other words, it functions as a virtual impedance. This indicates that the appropriate selection of droop gain achieves proportionate current sharing across all DGs.

3. Objective of work

Proportionate power sharing amongst all distributed energy resources is accomplished in the droop control method for the primary level. If selecting a droop gain is significantly greater than a resistance of line and satisfies the above Equation 8. Examining Equation 4, we can see that if a converter output current is more than zero, DC bus voltage represented by V_{bus} will be different from its nominal voltage represented by V_b^* .

Further, the voltage deviation ($V_b^* - V_{bus}$) increases with increasing droop gain R_{di} . Therefore, the key objective of this

paper is to maintain the accuracy of current sharing and simultaneously restore a DC bus voltage equal to its nominal voltage.

4. Principle of Proposed Secondary Control

Figure 2 displays a block arrangement for the proposed control techniques. It is a secondary-level control of a DC microgrid. Here, a low bandwidth communication network is built by using a Controller Area Network (CAN) bus, and for the DC-DC interface, buck converters are employed. Two distinct controllers make up the control method. A primary controller and a secondary controller. An outer loop droop control, an inner loop current control, and an inner loop voltage control make up a primary level control. Every converter's DC output voltage has been regulated through an inner-loop control. A droop control generates the reference signal for an inner loop control to provide proportionate current distribution amongst all converters.

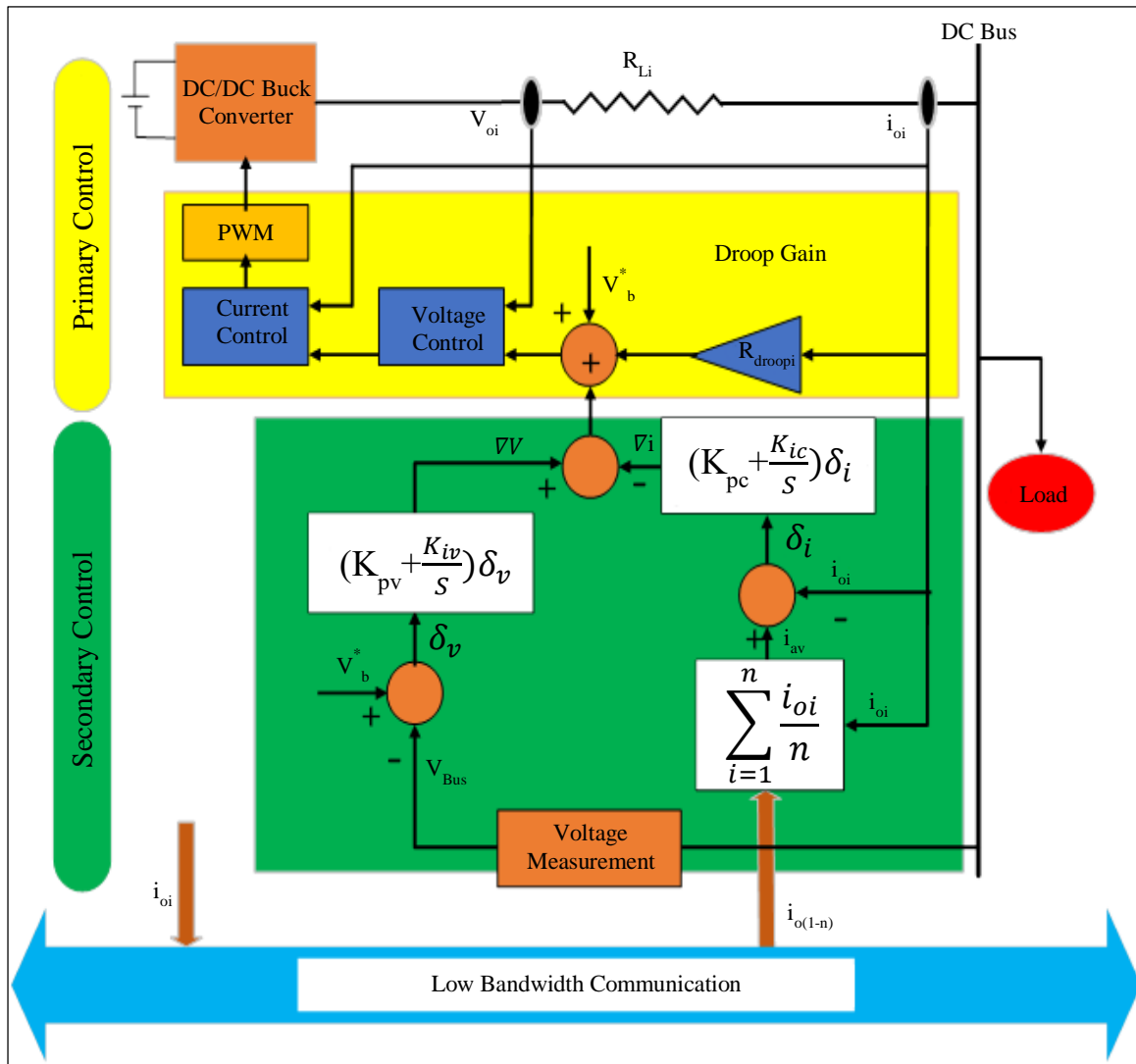


Fig. 2 Proposed secondary control

Across low bandwidth communication channels, all converter output current is communicated to all other converters. In the meantime, each converter receives the voltage of the DC bus. There are two control loops in the secondary control layer. A current control loop to control a current and a voltage control loop to control a voltage. In a current control loop, first compute the average current i_{av} . After that, the current signal δi is generated by comparing the average current and the converter's output current. Meanwhile, a voltage control loop compares the reference voltage and a DC bus voltage in order to generate a voltage signal, δv .

Meanwhile, a voltage control loop compares a reference voltage and voltage of a DC bus in order to generate a voltage signal, δv . These signals of voltage and current go via two PI (Proportional Integral) controllers to generate the voltage errors Δv and current errors Δi . The secondary level control produced the reference signal for the primary level droop control.

The secondary level voltage loop control is responsible for restoring the voltage of the DC bus back to its reference or nominal voltage. The secondary current controller ensures proportionate load current sharing amongst all converters. Since all computations are carried out locally, the proposed approach can be applied to distributed secondary control in a DC microgrid. The following equation represents the proposed secondary control method.

$$V_{dci}^* = V_b^* - R_{di}i_{oi} + \Delta V - \Delta \tag{9}$$

$$\Delta V = \left(K_{pv} + \frac{K_{iv}}{s} \right) (V_b^* - V_{bus}) \tag{10}$$

$$\Delta i = \left(K_{pc} + \frac{K_{ic}}{s} \right) (i_{av} - I_{oi}) \tag{11}$$

Where V_{dci}^* is represents the reference voltage of an i^{th} converters, V_b^* is represents the reference voltage of a DC bus, R_{di} is an i^{th} converter droop coefficient, K_{ic} and K_{pc} are the integration and proportional gain of the PI controller in a secondary-level current control loop and K_{iv} and K_{pv} are the integration and proportional gain of the PI controller in a secondary-level voltage control loop.

5. Simulation Result

MATLAB/SIMULINK software is utilized to prove the efficiency of a droop control at the primary level and proposed control techniques at the secondary level. A block arrangement for a simulation is presented in Figure 3. It comprises two buck converters that are parallelly connected to supply the load connected to the common bus. The system parameters are as per Table 1. The line 1 resistance is 0.02 ohm, and the line 2 resistance is 0.08 ohm.

5.1. Primary (Droop) Control

The study explores the performance of a droop control at the primary control under different resistive load conditions. The following four stages are used to energize the DC microgrid system:

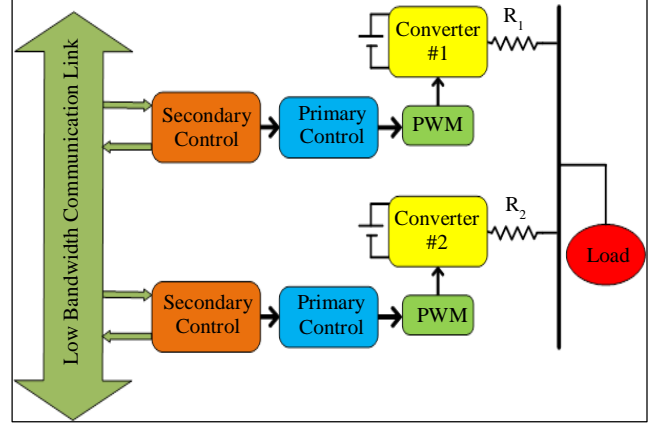


Fig. 3 Simulation block diagram

Table 1. Parameter of DC microgrid

Parameter	Converter-1	Converter-2
Power Rating	20 kW	20 kW
Output Voltage	400 Volt	400 Volt
Switching Frequency	10 kHz	10 kHz
Inductor	2.64 mH	2.64 mH
Capacitor	312.5 μF	312.5 μF
Line Resistance	0.02 Ω	0.08 Ω
Droop Gain	0.5	1
Secondary Voltage Loop	$K_{pv} = 50$	$K_{pv} = 50$
	$K_{iv} = 7$	$K_{iv} = 7$
Secondary Current Loop	$K_{pc} = 40$	$K_{pc} = 40$
	$K_{ic} = 7$	$K_{ic} = 7$

- Stage 1 (0-0.5 sec): At t = 0 seconds, connect a 10 kW load.
- Stage 2 (0.5-1 sec): At t = 0.5 seconds, increase the load to 20 kW.
- Stage 3 (1-1.5 sec): At t = 1 second, increase the load to 30 kW.
- Stage 4 (1.5-2 sec): At t = 1.5 seconds, increase the load to 40 kW.

Figure 4 displays the converter's output current, and Figure 5 displays the load current with a small droop gain ($R_{d1} = R_{d2} = 0.1$) and a large droop gain ($R_{d1} = R_{d2} = 1$), respectively, when primary control is applied.

Figure 4 shows that when the droop gain ($R_{d1} = R_{d2} = 0.1$) is taken into account, converter-1's output current, represented by i_1 , is about 14.53 A, and an output current of converter-2, represented by i_2 , is 10.32 A. The difference in an output current ($i_1 - i_2$) is approximately 4.21 A for a 10 kW load. The current i_1 is about 28.97 A, and the current i_2 is 20.47 A, and the difference in current ($i_1 - i_2$) is approximately 8.5 A for a 20 kW load. The current i_1 is about 43.23 A, and the current i_2 is 30.55 A, and the difference in current ($i_1 - i_2$) is approximately 12.68 A for a 30 kW load. The current i_1 is about 57.32 A, and the current i_2 is 40.55 A, and the difference in current ($i_1 - i_2$) is approximately 16.77 A for a 40 kW load. It shows the difference in an output current ($i_1 - i_2$) is very large. In comparison to the actual load-sharing condition, converter 1 shares a greater load and converter 2 shares a lesser load.

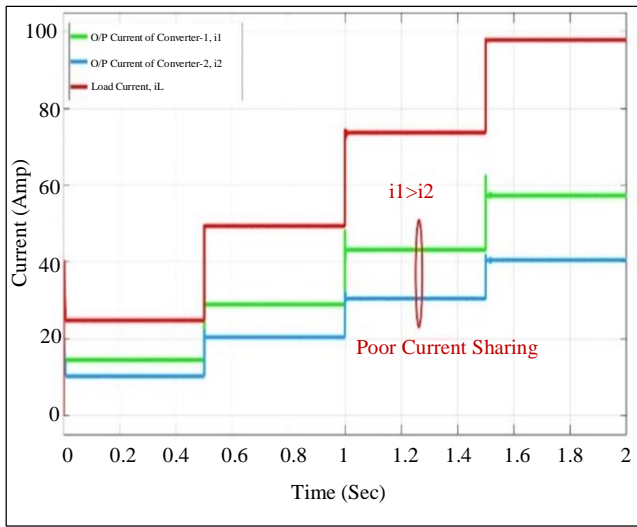


Fig. 4 Current with droop gain ($R_{d1} = R_{d2} = 0.1$)

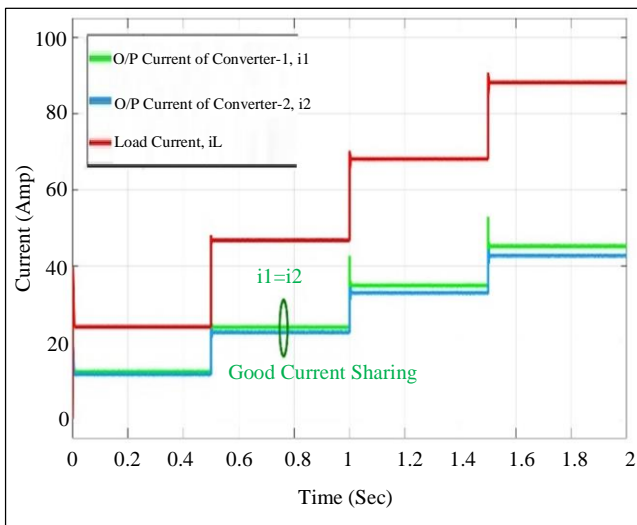


Fig. 5 Current with droop gain ($R_{d1} = R_{d2} = 1$)

Figure 5 shows that when the droop gain ($R_{d1} = R_{d2} = 1$) is taken into account converter-1's output current, represented by i_1 , is about 12.42 A, and an output current of converter-2, represented by i_2 , is 11.75 A. And the difference in an output current ($i_1 - i_2$) is approximately 0.67 A for a 10 kW load. The current i_1 is about 24.1 A, and the current i_2 is 22.75 A, and the difference in current ($i_1 - i_2$) is approximately 1.35 A for a 20 kW load.

The current i_1 is about 35.02 A, and the current i_2 is 33.1 A, and the difference in current ($i_1 - i_2$) is approximately 1.91 A for a 30 kW load, and the current i_1 is about 45.28 A, and the current i_2 is 42.83 A, and the difference in current ($i_1 - i_2$) is approximately 2.45 A for a 40 kW load. The difference in output current ($i_1 - i_2$) is very small compared to Figure 4. As a result, both converters almost share an equal load current.

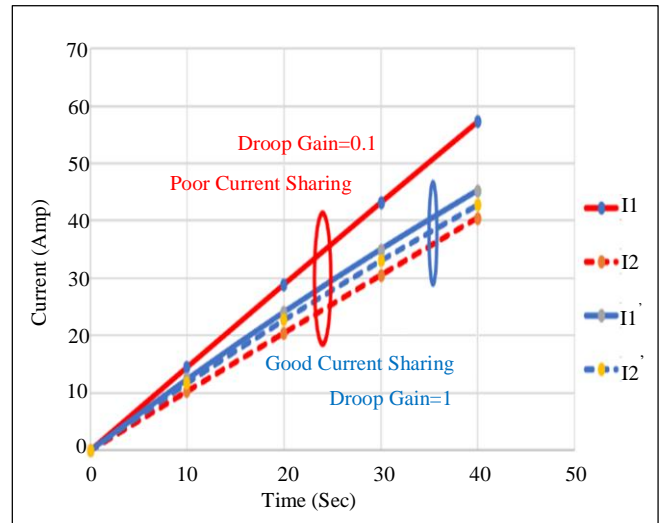


Fig. 6 Current sharing with different droop gains

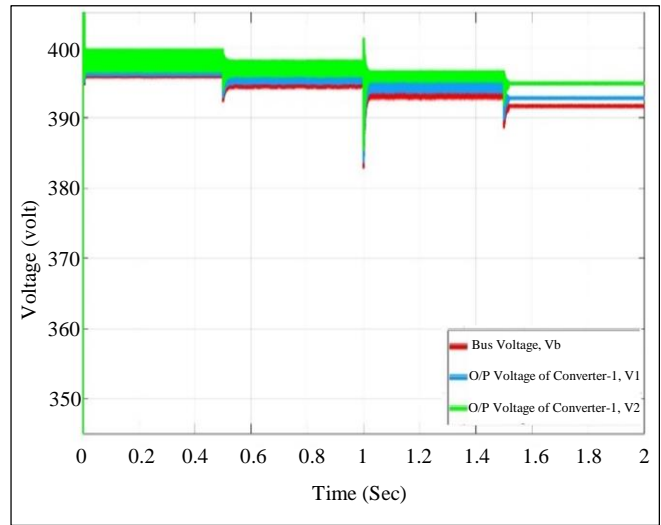


Fig. 7 Voltage with droop gain ($R_{d1} = R_{d2} = 0.1$)

Figure 6 displays load current sharing between both converters with a small droop gain ($R_{d1} = R_{d2} = 0.1$) and large droop gain ($R_{d1} = R_{d2} = 1$) with variable load from a condition of no load to a condition of full load. Where I_1 and I_2 represent the converters' output currents with a droop gain of ($R_{d1} = R_{d2} = 0.1$) and I_1' and I_2' for a droop gain of ($R_{d1} = R_{d2} = 1$).

According to Figure 6, current sharing accuracy is extremely low for droop gain ($R_{d1} = R_{d2} = 0.1$). There is a significant variance in the output current of both converters. The accuracy of current sharing is relatively good for droop gain ($R_{d1} = R_{d2} = 1$), as there is little variance in both converter output currents.

Figure 7 displays an output voltage, and Figure 8 displays the load voltage of converters with a small droop gain ($R_{d1} = R_{d2} = 0.1$) and a large droop gain ($R_{d1} = R_{d2} = 1$) respectively, when primary control is applied.

Figure 7 shows that when the droop gain ($R_{d1} = R_{d2} = 0.1$) is taken into account, the DC bus voltage V_b is about 395.8 V for a 10 kW load, about 394.5 V for a 20 kW load, about 393.12 V for a 30 kW load, and about 391.67 V for a 40 kW load. Under full load conditions, the voltage of DC bus V_b decreases from the 400 V nominal voltage to 8.33 V. Accordingly, 2.08% voltage regulation is achieved.

Figure 8 displays that when a droop gain of ($R_{d1} = R_{d2} = 0.1$) is taken into account, the DC bus voltage V_b is about 386.77 V for a 10 kW load, about 374.8 V for a 20 kW load, about 363.4 V for a 30 kW load, and about 352.63 V for a 40 kW load. Under full load conditions, DC bus voltage V_b decreases from its 400 V nominal value to 47.37 V. Accordingly, 11.08% voltage regulation is achieved, which is very large compared to Figure 7.

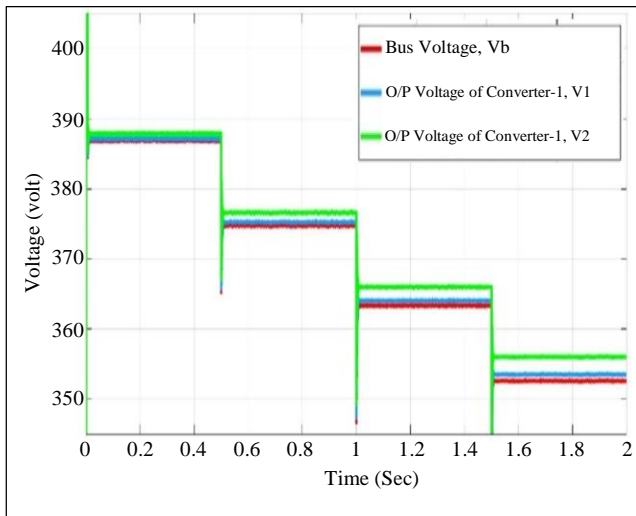


Fig. 8 Voltage with droop gain ($R_{d1} = R_{d2} = 1$)

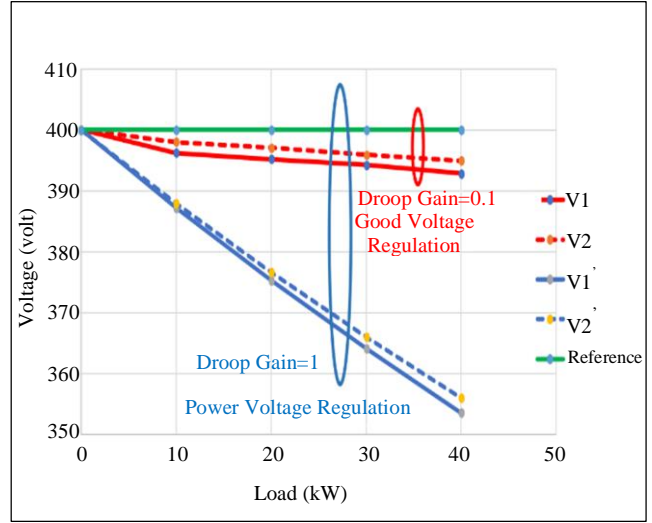


Fig. 9 Voltage regulation with different droop gains

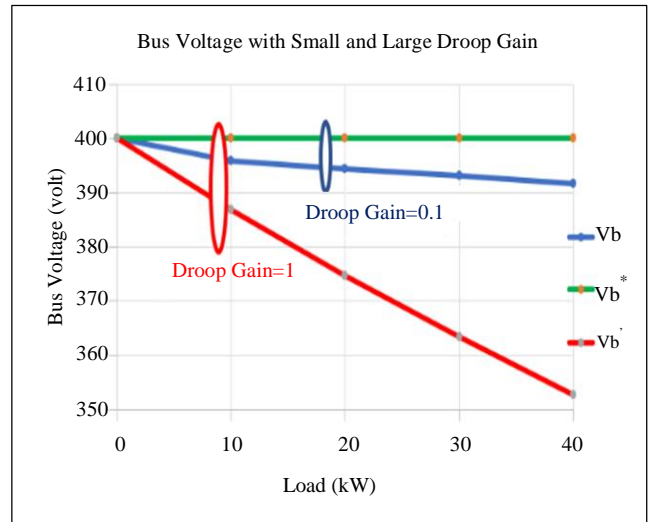


Fig. 10 Bus voltage with different droop gains

According to Figure 9, voltage regulation is relatively good for droop gain ($R_{d1} = R_{d2} = 0.1$) since there is little difference in the converter's output voltage from its nominal value. Voltage regulation is poor for droop gain ($R_{d1} = R_{d2} = 1$), as there is a significant variance in the converter's output voltage from its nominal value.

Figure 10 shows DC bus voltage with an increase in load for small droop gain ($R_{d1} = R_{d2} = 0.1$) and large droop gain ($R_{d1} = R_{d2} = 1$). Where V_b^* denotes a nominal voltage of a DC bus, V_b & V_b' denotes a voltage of a DC bus for a respectively $R_d=0.1$ and $R_d=1$ droop gain. As shown in Figure 10, a DC bus voltage is slightly reduced from its nominal value for small droop gain ($R_{d1} = R_{d2} = 0.1$) and greatly reduced from the nominal voltage for large droop gain ($R_{d1} = R_{d2} = 1$). Furthermore, DC bus voltage reduces very much with an increase in load.

5.2. Proposed Secondary Control

This section employs three different case studies to validate the efficiency of a proposed distributed secondary control technique. The control scheme with an increase in resistive load is tested in the first study. A decrease in resistive load is tested in the second study, and the third study tested for a variable resistive load.

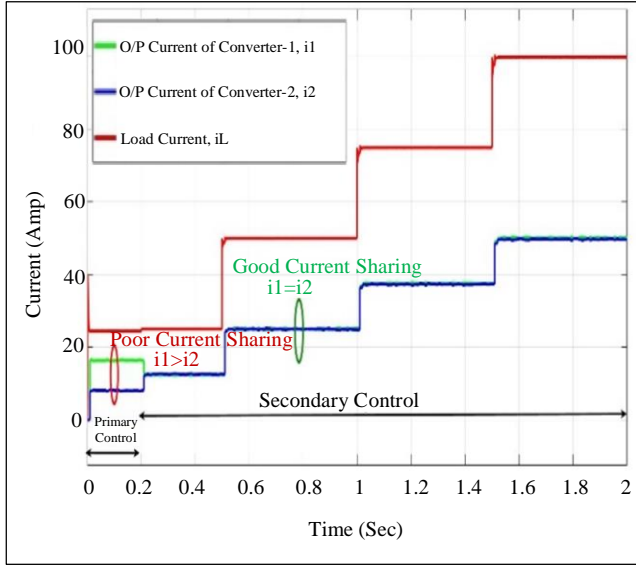


Fig. 11 Current with an increase in load

Current i_1 is around 25.01 A, and current i_2 is 24.98 A for a 20 kW load. Current i_1 is 37.62 A, and current i_2 is 37.22 A for a 30 kW load. And current i_1 is 50.18 A, and the current i_2 is 49.79 A for a 40 kW load. Both converters output currents are nearly equal under increasing load conditions, proving that the current sharing accuracy is greatly increasing.

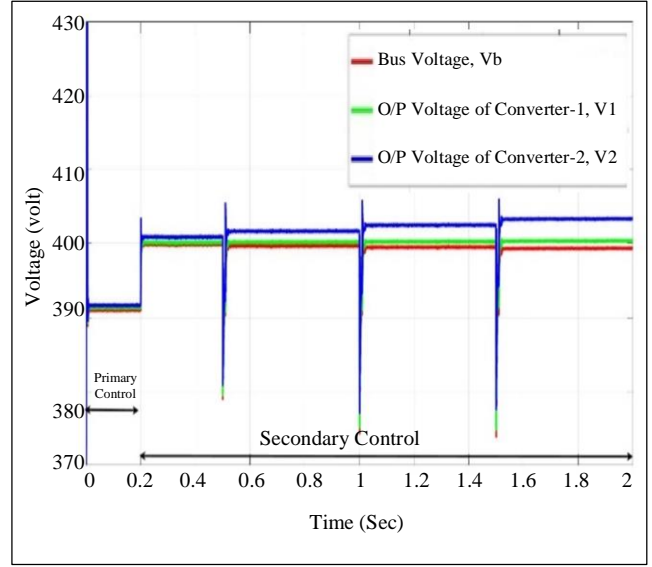


Fig. 12 Voltage with an increase in load

5.2.1. Case Study-I: Increase in Load

This study evaluates the function of the proposed distributed secondary control method under an increase in resistive load. The following 5 steps are used to energize the DC microgrid system.

- Step 1 (0-0.2 sec): Only droop control is used as primary control at $t = 0$ second with a 10 kW load.
- Step 2 (0.2-0.5 sec): At $t = 0.2$ seconds, the proposed secondary control is used
- Step 3 (0.5-1 sec): At $t = 0.5$ seconds, increase the load to 20 kW.
- Step 4 (1-1.5 sec): At $t = 1$ second, increase the load to 30 kW.
- Step 5 (1.5-2 sec): At $t = 1.5$ seconds, increase the load to 40 kW.

The case study I results are displayed in Figures 11 and 12. According to Figure 11, when only droop control is used for the first 0.2 seconds, the converter-1 output current given by i_1 is around 16.24 A, and the output of converter-2 given by i_2 is 8.22 A for a 10 kW load.

Converter 1 shares a greater load, and Converter 2 shares a lesser load than the definite load-sharing condition. The accuracy of current sharing at this time is quite low. When the proposed secondary control is implemented, the current i_1 is around 12.61 A, and the current i_2 is 12.56 A for a 10 kW load.

According to Figure 12, when only droop control is used for the first 0.2 seconds, the DC bus voltage decreases to around 392 V from a 400 V nominal voltage. The DC bus voltage is returned back to around 399.5 V when the proposed technique is implemented at 0.2 seconds. The DC bus voltage stays stable around a 400 V nominal value when the load is increased from 10 kW to 40 kW in a step of 10 kW.

5.2.2. Case Study-II: Decrease in Load

This study examines the function of a proposed distributed secondary control technique under the decrease in resistive load. The following 5 steps are used to energize the DC microgrid system.

- Step 1 (0-0.2 sec): Only droop control is used as primary control at $t = 0$ second with a 40 kW load.
- Step 2 (0.2-0.5 sec): At $t = 0.2$ seconds, the proposed secondary control is used.
- Step 3 (0.5-1 sec): At $t = 0.5$ seconds, decrease the load to 30 kW.
- Step 4 (1-1.5 sec): At $t = 1$ second, decrease the load to 20 kW.
- Step 5 (1.5- 2 sec): At $t = 1.5$ seconds, decrease the load to 10 kW.

Results of the case study II are displayed in Figures 13 and 14. According to Figure 13, when only droop control is used for the first 0.2 seconds, the converter-1 output current i_1

is around 61.03 A, and the output current of converter-2 i_2 is 30.02 A for a 40 kW load. Converter 1 shares a greater load, and converter 2 shares a lesser load than the definite load-sharing condition. The accuracy of current sharing at this time is very low.

When the proposed secondary control is implemented, the current i_1 is around 49.9 A, and the current i_2 is 49.6 A for a 40 kW load. Current i_1 is around 37.6 A, and current i_2 is 37.1 A for a 30 kW load.

Current i_1 is 25.2 A, and current i_2 is 24.7 A for 20 kW and current i_1 is 12.9 A, and current i_2 is 12.2 A for 10 kW load. Both converters output currents are nearly equal under decreasing load conditions. Hence, the current sharing performance is greatly enhanced.

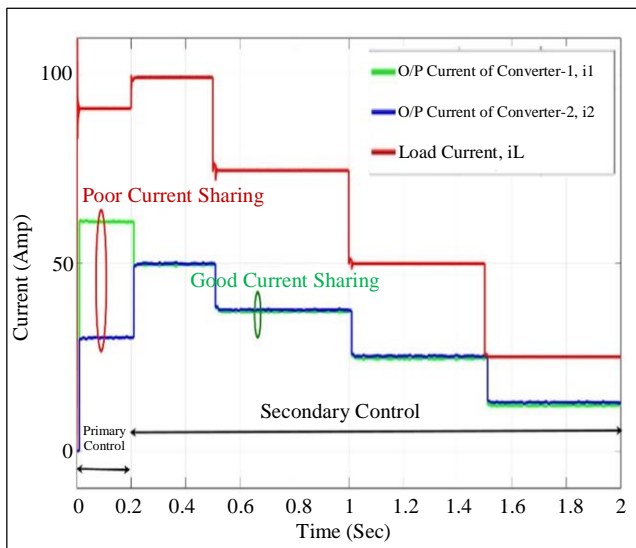


Fig. 13 Current with a decreased in load

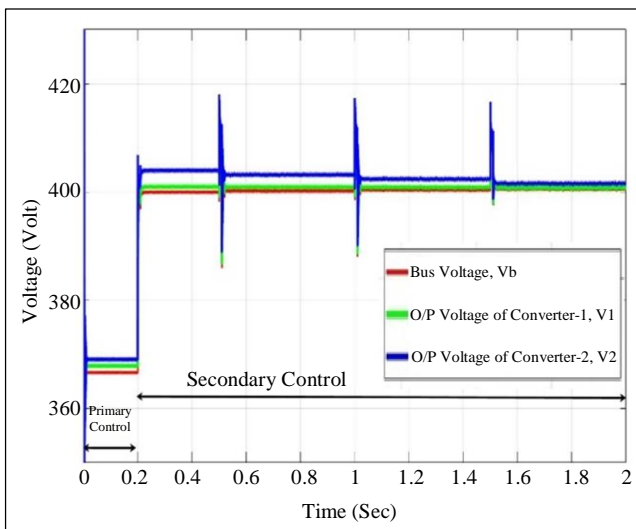


Fig. 14 Voltage with a decrease in load

According to Figure 14, when only droop control is used for the first 0.2 seconds, the DC bus voltage is reduced to around 366.65 V from the nominal value of 400 V. The voltage of the DC bus is returned back to almost 399.4 V at 0.2 seconds when the proposed technique is implemented. The voltage of the DC bus maintains a stable around 400 V nominal voltage as the load decreases from 40 kW to 10 kW in a step of 10 kW.

5.2.3. Case Study- III: Variable Load

This study assesses the function of the proposed secondary control technique with a variable resistive load condition. The following 5 steps are employed to energize the DC microgrid system.

- Step 1 (0-0.2 sec): Only droop control is used as primary control at $t = 0$ second with a 10 kW load.
- Step 2 (0.2-0.5 sec): At $t = 0.2$ seconds, the proposed secondary control is activated.
- Step 3 (0.5-1 sec): At $t = 0.5$ seconds, increase the load to 40 kW.
- Step 4 (1-1.5 sec): At $t = 1$ second, decrease the load to 30 kW.
- Step 5 (1.5-2 sec): At $t = 1.5$ sec, decrease the load to 10 kW.

The case study III results are displayed in Figures 15 and 16. According to Figure 15, when only droop control is used for the first 0.2 seconds, the converter-1 output current, denoted by i_1 , is around 16.4 A, and the output current of Converter-2 denoted by i_2 is 8.11 A for a 10 kW load. Converter 1 shares a greater load, and converter 2 shares a lesser load than the definite load-sharing condition.

The accuracy of current sharing at this time is quite low. When the proposed secondary control is implemented, the current i_1 is around 12.6 A, and the current i_2 is 12.5 A for a 10 kW load. Current i_1 is around 49.5 A, and current i_2 is 49.4 A for a 40 kW load.

Current i_1 is 37.4 A, and current i_2 is 37.2 A for a 30 kW load. Moreover, the current i_1 is 12.6 A, and the current i_2 is 12.5 A for a 10 kW load. Both converters output currents are nearly equal under variable load conditions. Hence, the accuracy of current sharing is greatly improved.

According to Figure 16, when only droop control is used for the first 0.2 seconds, the DC bus voltage is reduced to around 391 V from its 400 V nominal voltage. The DC bus voltage is back to around 399.6 V at 0.2 seconds when the proposed distributed secondary control method is implemented. The DC bus voltage remains stable around its 400 V nominal voltage for the variable load.

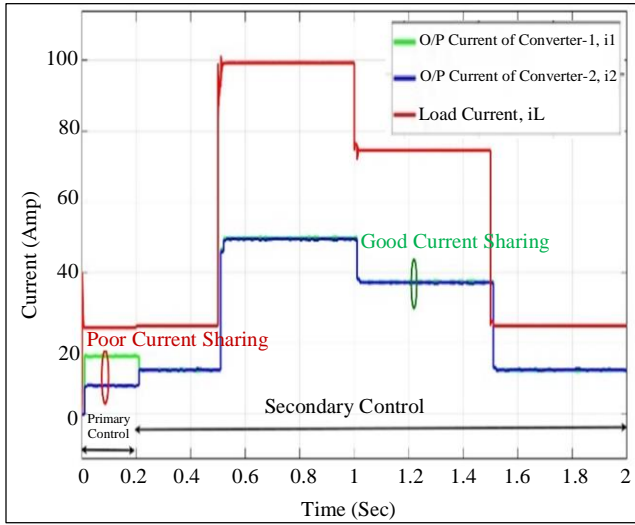


Fig. 15 Current with a variable load

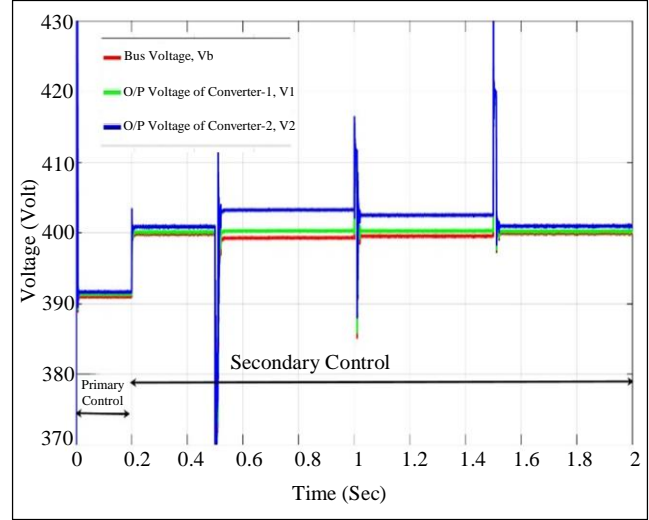


Fig. 16 Voltage with a variable load

6. Conclusion

This paper presents a low-bandwidth Communication Network (CAN) based distributed approach to secondary-level control in DC microgrids. At primary level control using a conventional droop controller, a DC bus voltage deviates less from its nominal voltage while using a smaller droop gain. However, the accuracy of current sharing is poor. Conversely, when selecting a large droop gain, the current sharing accuracy is highly improved, but the DC bus voltage significantly drops from the nominal voltage. Further, the voltage of the DC bus reduces greatly with an increase in load. When the proposed secondary control technique is

implemented, both converter output currents are nearly equal, which indicates that the load current is shared equally, whether it increases or decreases. The voltage of the DC bus returned to nearly 400 volts of its nominal voltage. That ensures proper current sharing among all converters, and the DC bus voltage remains stable at nominal voltage regardless of changes in load profile.

Future research will concentrate on expanding the proposed secondary control methodology by utilizing neighbour converter data for multi-converter microgrid applications.

References

- [1] Xia Chen et al., "Distributed Cooperative Control and Stability Analysis of Multiple DC Electric Springs in a DC Microgrid," *IEEE Transactions on Industrial Electronics*, vol. 65, no. 7, pp. 5611-5622, 2018. [[CrossRef](#)] [[Google Scholar](#)] [[Publisher Link](#)]
- [2] Pandla Chinna Dastagiri Goud, and Rajesh Gupta, "Solar PV Based Nanogrid Integrated with Battery Energy Storage to Supply Hybrid Residential Loads Using Single-Stage Hybrid Converter," *IET Energy Systems Integration*, vol. 2, no. 2, pp. 161-169, 2020. [[CrossRef](#)] [[Google Scholar](#)] [[Publisher Link](#)]
- [3] Babak Abdolmaleki et al., "An Instantaneous Event-Triggered Hz-Watt Control for Microgrids," *IEEE Transactions on Power Systems*, vol. 34, no. 5, pp. 3616-3625, 2019. [[CrossRef](#)] [[Google Scholar](#)] [[Publisher Link](#)]
- [4] Estefanía Planas et al., "AC and DC Technology in Microgrids: A Review," *Renewable and Sustainable Energy Reviews*, vol. 43, pp. 726-749, 2015. [[CrossRef](#)] [[Google Scholar](#)] [[Publisher Link](#)]
- [5] Jayendra Kumar, Anshul Agarwal, and Nitin Singh, "Design, Operation and Control of a Vast DC Microgrid for Integration of Renewable Energy Sources," *Renewable Energy Focus*, vol. 34, pp. 17-36, 2020. [[CrossRef](#)] [[Google Scholar](#)] [[Publisher Link](#)]
- [6] K.R. Bharath, M. Krishnan Mithun, and P. Kanakasabapathy, "A Review on DC Microgrid Control Techniques, Applications and Trends," *International Journal of Renewable Energy Research*, vol. 9, no. 3, pp. 1328-1338, 2019. [[Google Scholar](#)] [[Publisher Link](#)]
- [7] Lexuan Meng et al., "Review on Control of DC Microgrids and Multiple Microgrid Clusters," *IEEE Journal of Emerging and Selected Topics in Power Electronics*, vol. 5, no. 3, pp. 928-948, 2017. [[CrossRef](#)] [[Google Scholar](#)] [[Publisher Link](#)]
- [8] Zhikang Shuai et al., "Characteristics and Restraining Method of Fast Transient Inrush Fault Currents in Synchronverters," *IEEE Transactions on Industrial Electronics*, vol. 64, no. 9, pp. 7487-7497, 2017. [[CrossRef](#)] [[Google Scholar](#)] [[Publisher Link](#)]
- [9] Junbin Fang et al., "Secondary Power Sharing Regulation Strategy for a DC Microgrid via Maximum Loading Factor," *IEEE Transactions on Power Electronics*, vol. 34, no. 12, pp. 11856-11867, 2019. [[CrossRef](#)] [[Google Scholar](#)] [[Publisher Link](#)]
- [10] Qi-Fan Yuan et al., "Distributed Fixed-Time Secondary Control for DC Microgrid via Dynamic Average Consensus," *IEEE Transactions on Sustainable Energy*, vol. 12, no. 4, pp. 2008-2018, 2021. [[CrossRef](#)] [[Google Scholar](#)] [[Publisher Link](#)]

- [11] Waner Wodson A.G. Silva, Thiago R. Oliveira, and Pedro F. Donoso-Garcia, "An Improved Voltage-Shifting Strategy to Attain Concomitant Accurate Power Sharing and Voltage Restoration in Droop-Controlled DC Microgrids," *IEEE Transactions on Power Electronics*, vol. 36, no. 2, pp. 2396-2406, 2021. [[CrossRef](#)] [[Google Scholar](#)] [[Publisher Link](#)]
- [12] Lantao Xing et al., "Distributed Secondary Control for DC Microgrid with Event-Triggered Signal Transmissions," *IEEE Transactions on Sustainable Energy*, vol. 12, no. 3, pp. 1801-1810, 2021. [[CrossRef](#)] [[Google Scholar](#)] [[Publisher Link](#)]
- [13] Josep M. Guerrero et al., "Hierarchical Control of Droop-Controlled AC and DC Microgrids - A General Approach toward Standardization," *IEEE Transactions on Industrial Electronics*, vol. 58, no. 1, pp. 158-172, 2011. [[CrossRef](#)] [[Google Scholar](#)] [[Publisher Link](#)]
- [14] Made Andik Setiawan, Ahmed Abu-Siada, and Farhad Shahnia, "A New Technique for Simultaneous Load Current Sharing and Voltage Regulation in DC Microgrids," *IEEE Transactions on Industrial Informatics*, vol. 14, no. 4, pp. 1403-1414, 2018. [[CrossRef](#)] [[Google Scholar](#)] [[Publisher Link](#)]
- [15] Xiaonan Lu et al., "State-of-Charge Balance Using Adaptive Droop Control for Distributed Energy Storage Systems in DC Microgrid Applications," *IEEE Transactions on Industrial Electronics*, vol. 61, no. 6, pp. 2804-2815, 2014. [[CrossRef](#)] [[Google Scholar](#)] [[Publisher Link](#)]
- [16] Mahmoud Saleh, Yusef Esa, and Ahmed A. Mohamed, "Communication-Based Control for DC Microgrids," *IEEE Transactions on Smart Grid*, vol. 10, no. 2, pp. 2180-2195, 2019. [[CrossRef](#)] [[Google Scholar](#)] [[Publisher Link](#)]
- [17] Anuoluwapo Aluko et al., "Advanced Distributed Cooperative Secondary Control of Islanded DC Microgrids," *Energies*, vol. 15, no. 11, pp. 1-17, 2022. [[CrossRef](#)] [[Google Scholar](#)] [[Publisher Link](#)]
- [18] Fanghong Guo et al., "Decentralized Communication-Free Secondary Voltage Restoration and Current Sharing Control for Islanded DC Microgrids," *IECON 2019 - 45th Annual Conference of the IEEE Industrial Electronics Society*, Lisbon, Portugal, pp. 6515-6520, 2019. [[CrossRef](#)] [[Google Scholar](#)] [[Publisher Link](#)]
- [19] Sandeep Anand, Baylon G. Fernandes, and Josep Guerrero, "Distributed Control to Ensure Proportional Load Sharing and Improve Voltage Regulation in Low-Voltage DC Microgrids," *IEEE Transactions on Power Electronics*, vol. 28, no. 4, pp. 1900-1913, 2013. [[CrossRef](#)] [[Google Scholar](#)] [[Publisher Link](#)]
- [20] Po-Hsu Huang et al., "A Novel Droop-Based Average Voltage Sharing Control Strategy for DC Microgrids," *IEEE Transactions on Smart Grid*, vol. 6, no. 3, pp. 1096-1106, 2015. [[CrossRef](#)] [[Google Scholar](#)] [[Publisher Link](#)]
- [21] Fei Gao et al., "An Improved Voltage Compensation Approach in a Droop-Controlled DC Power System for the More Electric Aircraft," *IEEE Transactions on Power Electronics*, vol. 31, no. 10, pp. 7369-7383, 2016. [[CrossRef](#)] [[Google Scholar](#)] [[Publisher Link](#)]
- [22] Rohit Kumar, and Mukesh K. Pathak, "Distributed Droop Control of DC Microgrid for Improved Voltage Regulation and Current Sharing," *IET Renewable Power Generation*, vol. 14, no. 13, pp. 2499-2506, 2020. [[CrossRef](#)] [[Google Scholar](#)] [[Publisher Link](#)]
- [23] Rohit Kumar, and Mukesh Kumar Pathak, "Control of DC Microgrid for Improved Current Sharing and Voltage Regulation," *2020 3rd International Conference on Energy, Power and Environment: Towards Clean Energy Technologies*, Meghalaya, India, pp. 1-4, 2021. [[CrossRef](#)] [[Google Scholar](#)] [[Publisher Link](#)]
- [24] Panbao Wang et al., "An Improved Distributed Secondary Control Method for DC Microgrids with Enhanced Dynamic Current Sharing Performance," *IEEE Transactions on Power Electronics*, vol. 31, no. 9, pp. 6658-6673, 2016. [[CrossRef](#)] [[Google Scholar](#)] [[Publisher Link](#)]
- [25] Lantao Xing et al., "Voltage Restoration and Adjustable Current Sharing for DC Microgrid with Time Delay via Distributed Secondary Control," *IEEE Transactions on Sustainable Energy*, vol. 12, no. 2, pp. 1068-1077, 2021. [[CrossRef](#)] [[Google Scholar](#)] [[Publisher Link](#)]